The frequency response of temperature and precipitation in a climate model

Douglas G. MacMynowski,[1] Ho-Jeong Shin,[2] and Ken Caldeira[2]

Received 22 June 2011; revised 20 July 2011; accepted 21 July 2011; published 25 August 2011.

[1] Dynamic aspects of the climate's response to forcing are typically explored through transient simulations in the time domain. However, because of the large range of time-scales involved, some features are more easily observed in the frequency domain. We compute the frequency-response of the HadCM3L general circulation model (GCM) to sinusoidal perturbations in solar radiative forcing, with periods between $2^{-1/2}$ and 2^{9} (512) years. The global mean temperature response decreases with increasing frequency, and the frequency scaling at time-scales longer than one year is consistent with the behavior of diffusion into a semi-infinite slab. The land-sea contrast and land-averaged precipitation, however, exhibit relatively little dependency on the frequency of the imposed perturbation, with significant response at both short and long periods. Understanding these relative characteristics of different climate variables in the frequency domain is important to understanding the transient response of the climate system to both anthropogenic and natural (e.g., volcanic) forcings; the frequency response is also relevant in understanding the spectrum of natural variability.
Citation: MacMynowski, D. G., H.-J. Shin, and K. Caldeira (2011), The frequency response of temperature and precipitation in a climate model, *Geophys. Res. Lett.*, *38*, L16711, doi:10.1029/2011GL048623.

1. Introduction

[2] Time-scales in the climate's response to radiative forcing perturbations range from weeks (atmosphere) to a few years (ocean mixed layer) to centuries and longer (deep ocean, cryosphere). Predicting climate change depends on understanding the effects of processes that occur on this wide range of timescales [*Hansen et al.*, 1985; *Manabe et al.*, 1991], yet a simple description of the response is useful for policy analysis [*Socolow and Lam*, 2007]. Several analyses [e.g., *Bala et al.*, 2010; *Held et al.*, 2010] have distinguished between fast and slow responses, but the true response involves many different time-scales; this wide range of scales makes it useful to explore the response in the frequency domain. Understanding the forced response as a function of frequency also yields insight into the spectra of natural variability [e.g., *Fraedrich and Blender*, 2003; *Huybers and Curry*, 2006]. The similar frequency dependence of the forced response and natural variability spectrum suggest that the latter may be the result of radiative forcing perturbations that are nearly white over a wide range of time-scales, as conjectured by *Fraedrich et al.* [2004].

[3] We conducted simulations with the HadCM3L fully-coupled atmosphere-ocean GCM to explore the forced response of the climate system due to sinusoidal perturbations in radiative forcing, introduced here by varying the total solar irradiance (TSI) with periods from $2^{-1/2}$ to 512 years. Some of these results have been used in understanding the signal to noise ratio for geoengineering (D. G. MacMynowski et al., Can we test geoengineering?, submitted to *Royal Society Journal of Energy and Environmental Science*, 2011). Rather than present a comprehensive summary of the frequency-response of every climate field, we have chosen to focus on only a few key fields that are relevant to climate projections and illustrate important effects: the global mean surface air temperature, spatial dependence of temperature, land-sea temperature contrast, and land-averaged precipitation.

2. Simulations and Analysis

[4] The HadCM3L model resolution is 3.75° in longitude by 2.5° in latitude in both the atmosphere and ocean, with 19 vertical levels in the atmosphere and 20 in the ocean [*Jones*, 2003]. This has reduced ocean resolution compared to the more extensively used HadCM3, and similar climate sensitivity of 3°C. HadCM3L has climate variability similar to that of the real climate (MacMynowski et al., submitted manuscript, 2011), including capturing ENSO [*Jones et al.*, 2001]. At sufficiently long time-scales, other physics not captured in this model (ice-sheets, dynamic vegetation) will clearly change the frequency response. All simulations used pre-industrial greenhouse gas concentrations.

[5] Sinusoidal variations in TSI were introduced with a ±1% maximum variation. 1600, 1100 and 600 year simulations were used for the 512-, 256-, and 128-year cases respectively in order to obtain sufficient cycles of excitation, and 500 years were used for all shorter periods. The first 50 years were discarded to avoid initialization transients. The Fourier transform of monthly-averaged fields over an integer number of forcing cycles is used to compute the magnitude and phase of the response that is correlated with the forcing. Natural climate variability at the forcing frequency will result in some error in these response estimates; this is at most a 5% effect for the fields presented here. Responses are plotted per Wm^{-2} change in TSI.

[6] The sinusoidal perturbations have minimal effect on the mean climate, nor are there significant harmonics of the forcing frequency introduced. The phase of the forcing matters for a 2-year period; forcing that reaches its maxima and minima in northern hemisphere summer gives a different response from forcing that peaks in winter [cf. *Kravitz and Robock*, 2011]. We instead use a 449/225-year period to avoid phase-locking with the seasonal cycle. At 4-year and

[1]Control and Dynamical Systems, California Institute of Technology, Pasadena, California, USA.
[2]Department of Global Ecology, Carnegie Institution, Stanford, California, USA.

0094-8276/11/2011GL048623

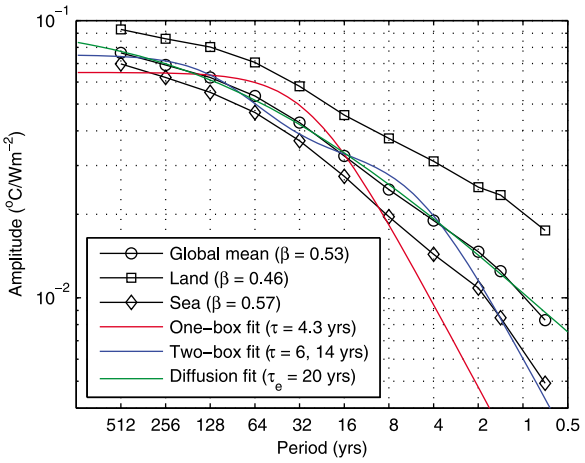

Figure 1. Temperature response to solar radiative forcing at different periods. The global mean response per Wm^{-2} change in TSI (black, circles) is compared to the best fit to a single-box (red), two-box (blue) and semi-infinite diffusion model (green); the last of these clearly gives the best fit. The time-constants for each model are given in the legend, for the diffusion model the time-scale given is $\tau_e = 1.56\tau$. The land- and ocean-average response are also plotted, and the slope β for a fit to $k/(1+(\tau f)^{\beta})$ is given in the legend; the slope is shallower over land than over ocean.

longer periods the correlated component evaluated here on monthly model output is nearly the same as evaluating the change in the annual mean climate that is correlated with the forcing.

3. Simple Models for Temperature Response

[7] Several simple models have been used to describe the frequency-dependent response of the global mean temperature to radiative forcing, starting with a single-reservoir energy balance model with heat capacity C and feedback λ:

$$C\frac{\mathrm{d}T}{\mathrm{d}t} = F - \lambda T \tag{1}$$

Taking the Laplace transform yields the complex-valued transfer function [e.g., *MacMynowski and Tziperman*, 2010; K. J. Åström and R. M. Murray, Feedback Systems: An Introduction for Scientists and Engineers, 2008, available at http://www.cds.caltech.edu/~murray/amwiki/index.php/Main_Page.] from forcing F (at frequency f) to temperature:

$$H_1(s) = \frac{1}{Cs+\lambda} \tag{2}$$

where $s = 2\pi i f$. The magnitude of H_1 gives the amplitude of the sinusoidal temperature response to a sinusoidal perturbation in radiative forcing, and the phase of H_1 gives the lead or lag of the response relative to the forcing.

[8] A two-box model [*Gregory*, 2000; *Held et al.*, 2010] has the potential to capture both the "fast" and "slow" response due to different parts of the system:

$$C\frac{\mathrm{d}T}{\mathrm{d}t} = F - \lambda T - \gamma(T - T_0), \qquad C_0\frac{\mathrm{d}T_0}{\mathrm{d}t} = \gamma(T - T_0) \tag{3}$$

[9] This yields the transfer function

$$H_2(s) = \frac{C_0 s + \gamma}{CC_0 s^2 + (\gamma C + (\lambda+\gamma)C_o)s + \lambda\gamma} \tag{4}$$

where C and C_0 are the heat capacities of the fast (ocean mixed layer) and slow (deep ocean) components, λ the feedback, and γ the coupling between surface and deep reservoirs. The equilibrium response is still $1/\lambda$, while for frequencies $1/C \gg 2\pi f \gg 1/C_0$ (where the fast response has equilibrated and the slow response is negligible), the transient climate sensitivity is $(\lambda+\gamma)^{-1}$. *Held et al.* [2010] estimate the fast time constant in the GFDL CM2.1 GCM as 3–4 years and the slow time-constant being many decades.

[10] Next consider heat diffusion into a semi-infinite medium with thermal diffusivity α and conductivity κ [*Oeschger et al.*, 1975; *Fraedrich et al.*, 2004]. Including a surface box of fixed heat capacity affects only the high-frequency behavior. The temperature depends on depth z as

$$\frac{\partial T}{\partial t} = \alpha\frac{\partial^2 T}{\partial z^2}, \qquad \kappa\frac{\partial T}{\partial z}\bigg|_{z=0} = F - \lambda T(t,0) \tag{5}$$

[11] The transfer function from forcing F to surface temperature $T(t, 0)$ is

$$H_3(s) = \frac{1}{\lambda + \kappa(s/\alpha)^{1/2}} \tag{6}$$

With $\tau = \kappa^2/(\lambda^2\alpha)$, the corresponding step response is

$$h_3(t) = \frac{1}{\lambda}\left(1 - e^{t/\tau}\mathrm{erfc}\left(\sqrt{t/\tau}\right)\right) \tag{7}$$

The response is within $1/e$ of its final value at $\tau_e = 1.56\tau$, but this system takes 10.5 times longer to reach within e^{-2} of the final value, and 81 times longer to reach within e^{-3}.

4. HadCM3L Response

[12] The frequency response of the HadCM3L global mean temperature is shown in Figure 1, including the fit to all three simple models (using only results for periods longer than 4 years). The legend gives the best-fit values for the single time-constant $\tau = C/\lambda$ in (1), the two time-constants for (3), and the time-scale $\tau_e = 1.56\tau$ for (6). The phase (see auxiliary material) is related to the magnitude by Bode's gain-phase relation (e.g., Åström and Murray, online textbook, 2008). Using the values of τ and λ estimated from the frequency response, (7) matches the step response of HadCM3L except at long time-scales (Figure 2); the behavior is similar to the two-box model for the first 50 years. Figure 1 also includes the frequency response for the land- and ocean-averaged temperature. The slope of the frequency dependence is estimated from the fit to

$$H_4(s) = \frac{1/\lambda}{1 + (\tau s)^{\beta}} \tag{8}$$

which has been used to describe variability [*Blender and Fraedrich*, 2006]. The slope here is shallower over land than ocean, consistent with the observed frequency-dependence of variability; the power spectrum is approximately $1/f$ (amplitude $f^{-1/2}$) but also shallower over land than

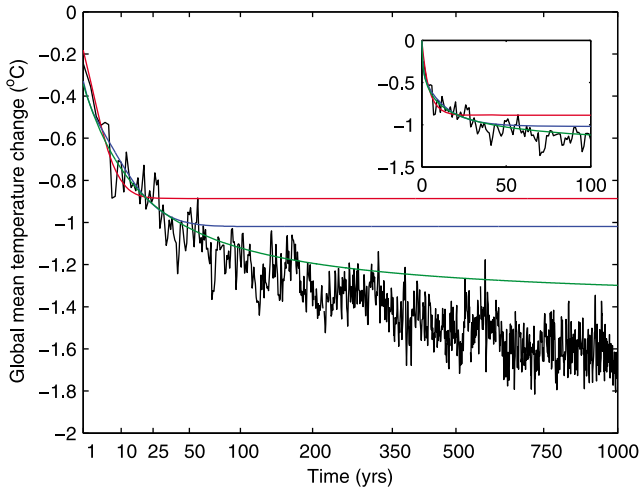

Figure 2. Global mean temperature (cooling) response to a 1% step decrease in TSI; both the baseline and step response are averaged over three simulations. The horizontal axis is linear in the square root of time. The step response of the one-box (red), two-box (blue) and semi-infinite diffusion models (green) are shown, with parameters fit from the frequency response. The inset shows the first 100 years on a linear time-scale; the diffusion and two-box models are almost indistinguishable for the first 50 years. Obtaining a better fit at long time scales would require estimating the frequency response at even lower frequencies (longer periods) than used here.

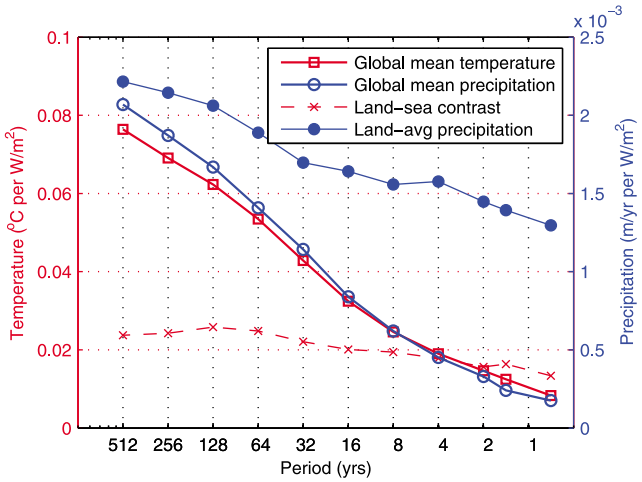

Figure 4. Frequency response comparing global precipitation (right axis) and temperature (left axis). The axes scaling is chosen to emphasize that the global mean precipitation response follows the global mean temperature (both shown with open symbols, thick lines). However, the land-average precipitation frequency response (solid circles) at short periods is closer in behavior to the land-sea contrast frequency response (difference between land- and ocean-average temperature, shown dashed, '×'). The ratio of land-averaged precipitation to temperature response is thus much larger at short period forcing than at long.

ocean. A consequence of this difference is that the land-sea contrast exhibits relatively little frequency dependence. A flat frequency response corresponds to a time constant shorter than the periods considered here, consistent with *Dong et al.* [2009]. This is important in influencing the precipitation response.

[13] The spatial characteristics of the frequency response also illustrate important insights. At short periods the response is primarily over land, while at long periods the largest response is in the arctic (Figure 3). The fit to (8) can be computed at each grid-point (see auxiliary material); some regions have a slope β significantly different from the value of 1/2 corresponding to diffusion. The time-scale is higher over ocean than over land, and can be significantly higher in regions where the surface ocean communicates with the deep ocean. Due to the prevailing wind direction, western regions of continents tend to be closer to oceanic values of τ and β, and western regions of oceans closer to continental values, similar to the observed seasonal cycle [*Stine et al.*, 2009].

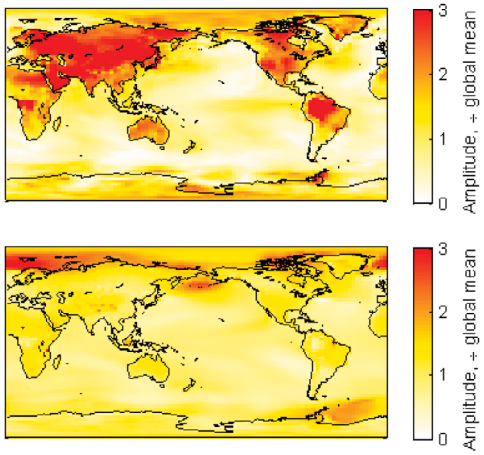

Figure 3. Spatial pattern of temperature response at a forcing period of (top) $2^{-1/2}$ and (bottom) 512 years, each normalized by the global mean temperature response at that period. At short periods, the response is primarily over land; at long periods the largest response is in the arctic.

[14] While the decreased temperature response at increased frequency is expected, not all fields respond the same way, as is evident from the land-sea contrast. The global mean precipitation is proportional to the global mean temperature (from Clausius-Clapeyron). However, the land-averaged precipitation response is markedly different (Figure 4), as it is influenced by the land-sea temperature contrast. The ratio of changes in the land-average precipitation to changes in temperature thus increases with frequency. The precipitation response at a 2-year period also depends on the phase of the forcing; at some phases, regional responses can be even larger than in steady-state (MacMynowski et al., submitted manuscript, 2011).

5. Discussion

[15] To our knowledge, this is the first explicit calculation using a fully-coupled GCM of the frequency response of key climate parameters to radiative forcing perturbations. Any time-varying perturbation can be expressed as a sum of its frequency components, so the frequency response provides a useful way to explore the system behavior. While this information differs from the time-domain response only

through a Fourier transform, understanding the frequency response is useful for illustrating several aspects of climate dynamics.

[16] For a wide range of forcing frequencies f, the global mean temperature response in this model scales as $f^{-1/2}$. This is consistent with a (one-dimensional) semi-infinite diffusion model [*Oeschger et al.*, 1975; *Hansen et al.*, 1985; *Fraedrich et al.*, 2004], rather than one- or two-box energy balance models often used in simple analyses. This is relevant in obtaining simple descriptions to estimate warming from different profiles of greenhouse gas concentrations. A single-box model is clearly inadequate for understanding climate response, see e.g., the responses of *Robock* [2005], *Wigley et al.* [2005], and *Knutti et al.* [2008] to the analyses of *Douglass and Knox* [2005] and *Schwartz* [2007]. A two-box model [*Gregory*, 2000; *Held et al.*, 2010] may be adequate, since for century-scale integrations it is difficult to distinguish from the diffusion model suggested by the results herein. However, the temperature in the diffusion model will continue to rise for centuries after the 2-box model has reached equilibrium. With the diffusion model, the time here to reach within $1/e$ of the equilibrium value is of order 20 years, but ten times longer to reach within $1/e^2$. Fitting the frequency response with a two-box model, the time to reach within $1/e$ (of the smaller estimated equilibrium value) is 7 years, and three times longer to reach within $1/e^2$.

[17] The frequency-domain analysis illustrates different qualitative characteristics for different variables. Both the magnitude and phase of the response differ between land and ocean. This results in the land-sea temperature contrast having a relatively flat frequency response over the time-scales considered herein, with almost as large a response to short-period forcing as to long. In the time domain, this corresponds to much of the response to changes in forcing occurring in less than a year. The land/atmosphere system equilibrates to SST changes on a subannual time scale, but it takes decades for the ocean to respond. The land response is thus driven by the time scale of the ocean, while the contrast between them is driven by the much shorter time constants of the land/atmosphere system [*Joshi et al.*, 2008; *Dong et al.*, 2009]. Since land-sea contrast influences precipitation over land (e.g., through influence over monsoonal circulation), this is an important factor in the land-averaged precipitation also having a relatively flat frequency response and corresponding rapid response to perturbations [see also *Dong et al.*, 2009; *Bala et al.*, 2010]. The land-average precipitation is also influenced by changes in the global mean temperature, which is the dominant factor at low frequencies. The differences in the frequency response of different parts of the climate system means that the response to a forcing consisting mostly of high-frequency components (e.g., volcanic eruptions) can have quite different characteristics from the response to slow changes (e.g., greenhouse gases); relevant in extrapolating effects from short-period to long-period forcing [*Trenberth and Dai*, 2007].

[18] The slope of the frequency response is similar to the spectrum of observed climate variability [*Fraedrich and Blender*, 2003; *Huybers and Curry*, 2006], suggesting that much of this variability may result from internally-generated radiative forcing perturbations that are close to white over these time-scales. While the global mean temperature scales with $f^{-1/2}$, the slope is higher over oceans than land, also consistent with the observed variability spectra. The relatively flat frequency response of land-averaged precipitation is again similar to the observed nearly white spectrum of natural variability at inter-decadal time-scales [*Blender and Fraedrich*, 2006]. Understanding natural variability is also relevant in understanding predictability [*Zhu et al.*, 2010].

[19] Finally, it is useful to compare the global mean temperature frequency response with estimates based on data. The response at 1-year forcing agrees with the estimated seasonal cycle response of $0.009°C/Wm^{-2}$ [*Laepple and Lohmann*, 2009]. The response at an 11-year period is much lower than some estimates of the solar cycle response, as high as $0.17\ °C/Wm^{-2}$ [*Tung and Camp*, 2008]. Constructing an empirical transfer function estimate [*MacMynowski and Tziperman*, 2010] from the historical record of temperature and radiative forcing (auxiliary material) is challenging due to the uncertainty in the latter, making it difficult either to compare the frequency response of this model, or to estimate the time-scale and hence climate sensitivity from this data alone.

[20] **Acknowledgments.** The Editor thanks Klaus Fraedrich and an anonymous reviewer.

References

Bala, G., K. Caldeira, and R. Nemani (2010), Fast versus slow response in climate change: Implications for the global hydrological cycle, *Clim. Dyn.*, *35*, 423–434.

Blender, R., and K. Fraedrich (2006), Long term memory of the hydrological cycle and river runoffs in China in a high resolution climate model, *Int. J. Climatol.*, *26*, 1547–1565.

Dong, B., J. M. Gregory, and R. T. Sutton (2009), Understanding land-sea warming contrast in response to increased greenhouse gases. Part I: Transient adjustment, *J. Clim.*, *22*, 3079–3097.

Douglass, D. H., and R. S. Knox (2005), Climate forcing by the volcanic eruption of Mount Pinatubo, *Geophys. Res. Lett.*, *32*, L05710, doi:10.1029/2004GL022119.

Fraedrich, K., and R. Blender (2003), Scaling of atmosphere and ocean temperature correlations in observations and climate models, *Phys. Rev. Lett.*, *90*, 108501.

Fraedrich, K., U. Luksch, and R. Blender (2004), $1/f$ model for long-time memory of the ocean surface temperature, *Phys. Rev. E*, *70*, 037301.

Gregory, J. M. (2000), Vertical heat transports in the ocean and their effect on time-dependent climate change, *Clim. Dyn.*, *16*, 501–515.

Hansen, J., G. Russel, A. Lacis, I. Fung, and D. Rind (1985), Climate response times: Dependence on climate sensitivity and ocean mixing, *Science*, *229*, 857–859.

Held, I. M., M. Winton, K. Takahashi, T. Delworth, F. Zeng, and G. V. Vallis (2010), Probing the fast and slow components of global warming by returning abruptly to preindustrial forcing, *J. Clim.*, *23*, 2418–2427.

Huybers, P., and W. Curry (2006), Links between annual, Milankovitch and continuum temperature variability, *Nature*, *441*, 329–332.

Jones, C. (2003), A fast ocean GCM without flux adjustments, *J. Atmos. Oceanic Technol.*, *20*, 1857–1868.

Jones, C. D., M. Collins, P. M. Cox, and S. A. Spall (2001), The carbon cycle response to ENSO: A coupled climate-carbon cycle model study, *J. Clim.*, *14*, 4113–4129.

Joshi, M. M., J. M. Gregory, M. J. Webb, D. M. H. Sexton, and T. C. Johns (2008), Mechanisms for the land/sea warming contrast exhibited by simulations of climate change, *Clim. Dyn.*, *30*, 455–465.

Knutti, R., S. Krähenmann, D. J. Frame, and M. R. Allen (2008), Comment on "Heat capacity, time constant, and sensitivity of Earth's climate system" by S. E. Schwartz, *J. Geophys. Res.*, *113*, D15103, doi:10.1029/2007JD009473.

Kravitz, B., and A. Robock (2011), Climate effects of high-latitude volcanic eruptions: Role of the time of year, *J. Geophys. Res.*, *116*, D01105, doi:10.1029/2010JD014448.

Laepple, T., and G. Lohmann (2009), Seasonal cycle as template for climate variability on astronomical timescales, *Paleoceanography*, *24*, PA4201, doi:10.1029/2008PA001674.

MacMynowski, D. G., and E. Tziperman (2010), Testing and improving ENSO models by process rather than by output, using transfer functions, *Geophys. Res. Lett.*, *37*, L19701, doi:10.1029/2010GL044050.

Manabe, S., R. J. Stouffer, M. J. Spelman, and K. Bryan (1991), Transient response of a coupled atmosphere-ocean model to gradual changes of atmospheric CO_2. Part I: Annual mean response, *J. Clim.*, *4*, 785–818.

Oeschger, H., U. Siegenthaler, U. Schotterer, and A. Gugelmann (1975), Box diffusion-model to study carbon-dioxide exchange in nature, *Tellus*, *27*(2), 168–192.

Robock, A. (2005), Comment on "Climate forcing by the volcanic eruption of Mount Pinatubo" by David H. Douglass and Robert S. Knox, *Geophys. Res. Lett.*, *32*, L20711, doi:10.1029/2005GL023287.

Schwartz, S. E. (2007), Heat capacity, time constant, and sensitivity of Earth's climate system, *J. Geophys. Res.*, *112*, D24S05, doi:10.1029/2007JD008746.

Socolow, R. H., and S. H. Lam (2007), Good enough tools for global warming policy making, *Philos. Trans. R. Soc. A*, *365*, 897–934.

Stine, A. R., P. Huybers, and I. Y. Fung (2009), Changes in the phase of the annual cycle of surface temperature, *Nature*, *457*, 435–441.

Trenberth, K. E., and A. Dai (2007), Effects of Mount Pinatubo volcanic eruption on the hydrological cycle as an analog of geoengineering, *Geophys. Res. Lett.*, *34*, L15702, doi:10.1029/2007GL030524.

Tung, K. K., and C. D. Camp (2008), Solar cycle warming at the Earth's surface in NCEP and ERA-40 data: A linear discriminant analysis, *J. Geophys. Res.*, *113*, D05114, doi:10.1029/2007JD009164.

Wigley, T. M. L., C. M. Ammann, B. D. Santer, and K. E. Taylor (2005), Comment on "Climate forcing by the volcanic eruption of Mount Pinatubo" by David H. Douglass and Robert S. Knox, *Geophys. Res. Lett.*, *32*, L20709, doi:10.1029/2005GL023312.

Zhu, X., K. Fraedrich, Z. Liu, and R. Blender (2010), A demonstration of long-term memory and climate predictability, *J. Clim.*, *23*, 5021–5029.

K. Caldeira and H.-J. Shin, Department of Global Ecology, Carnegie Institution, Stanford, CA 94065, USA.

D. G. MacMynowski, Control and Dynamical Systems, California Institute of Technology, 1200 E. California Blvd., M/C 107-81, Pasadena, CA 91125, USA. (macmardg@cds.caltech.edu)